Equilibrium and nonequilibrium molecular dynamics simulations of the thermal conductivity of molten alkali halides

N. Galamba and C. A. Nieto de Castro
Departamento de Química e Bioquímica e Centro de Ciências Moleculares e Materiais, Faculdade de Ciências da Universidade de Lisboa, 1749-016 Lisboa, Portugal

James F. Ely[a)]
Chemical Engineering Department, Colorado School of Mines, Golden, Colorado 80401-1887

(Received 7 December 2006; accepted 5 April 2007; published online 31 May 2007)

The thermal conductivity of molten NaCl and KCl was calculated through the Evans-Gillan nonequilibrium molecular dynamics (NEMD) algorithm and Green-Kubo equilibrium molecular dynamics (EMD) simulations. The EMD simulations were performed for a "binary" ionic mixture and the NEMD simulations assumed a pure system for reasons discussed in this work. The cross thermoelectric coefficient obtained from Green-Kubo EMD simulations is discussed in terms of the homogeneous thermoelectric power or Seebeck coefficient of these materials. The thermal conductivity obtained from NEMD simulations is found to be in very good agreement with that obtained through Green-Kubo EMD simulations for a binary ionic mixture. This result points to a possible cancellation between the neglected "partial enthalpy" contribution to the heat flux associated with the interdiffusion of one species through the other and that part of the thermal conductivity related to the coupled fluxes of charge and heat in "binary" ionic mixtures. © *2007 American Institute of Physics*. [DOI: 10.1063/1.2734965]

I. INTRODUCTION

Molten salts have been investigated experimentally and through theoretical and simulation methods for many years. The experimental difficulties associated with the measurement of the transport coefficients of these materials (e.g., high melting points and high chemical activity), however, limit the accuracy and range of these measurements. Thus, molecular dynamics (MD) simulations can play an important role in the study of properties such as the shear viscosity and the thermal conductivity of these substances.

Molten salts and ionic liquids in general are particularly interesting systems because of the marked differences observed in the chemical and physical properties of these systems as compared to normal fluids. These differences are closely related to the Coulombic long-range interactions and the electroneutrality condition, and the way these are manifested in the properties of different materials composed of particles of different sizes, shapes, valences, and masses. An especially interesting characteristic of molten salts is the fact that from Gibbs' phase rule, they are one-component systems composed of two different species which microscopically implies the occurrence of three different types of interactions, $++$, $+-$, and $--$. From this one-component thermodynamic definition, no thermal diffusion is expected to occur for a pure molten salt (as is the case for a one-component neutral system). The possibility of thermal diffusion in a 1:1 salt was investigated[1] through nonequilibrium molecular dynamics simulations as a function of the charge strength of the species and the range of the ionic potential. The results of that investigation showed that the Coulomb forces experienced by the ions inhibit thermal separation to any significant extent.

For solid or fused salts, and electrolytes in general, coupled thermoelectric effects occur. The application of a temperature gradient to an electrolyte leads to a flux of heat in the system and at the same time a potential difference develops in the material. This potential difference, ΔV, is related to the different mobilitities and heats of transport of the cations and the anions. This phenomenon is called the Seebeck effect and can be studied experimentally through the measurement of the electrical power of thermocells.

Experimentally the power of a thermocell, $\theta = \Delta V / \Delta T$, is approximately given by the sum of the homogeneous thermoelectric power intrinsic to the system and the heterogeneous thermoelectric power relating to the electrode-system interface.[2] Hence, solid and molten salts, and electrolytic solutions in general, are in a way more closely related to thermocouples than to binary mixtures. The inverse phenomenon, where an applied electric field leads to a charge flux and a temperature gradient, is characterized by the Peltier coefficient.

Using microcanonical (*NVE*) equilibrium molecular dynamics (EMD) simulation methods, we[3] have recently calculated the thermal conductivity for the Born-Mayer-Huggins-Tosi-Fumi[4–8] (BMHTF) rigid ion interionic potential model for molten NaCl and KCl. In that work the two molten salts were treated as "binary" ionic mixtures and no special attention was paid to the cross thermoelectric phenomenological coefficient that arises from the coupled fluxes of heat (energy) and charge. In this study we have calculated the thermal conductivity of the BMHTF po-

[a)]Author to whom correspondence should be addressed. FAX: 303-273-3730. Electronic mail: jely@mines.edu

tential for molten NaCl and KCl through both Green-Kubo EMD and nonequilibrium molecular dynamics (NEMD) simulations in the canonical ensemble where (N,V,T) are fixed. The EMD simulations were performed for a binary (1:1 salt) ionic mixture and the NEMD simulations assumed a pure system as discussed in Sec. III B. We also compare the thermoelectric coefficient obtained for the two fused salts and discuss it in terms of the Seebeck coefficient of these materials.

This paper is organized as follows: The methods and parameters used in the simulations are given in Sec. II. In Sec. III we derive relations for the thermal conductivity and the Seebeck coefficient from nonequilibrium thermodynamics for the case of a binary ionic mixture. In Sec. IV the calculation of the thermal conductivity through EMD in conjunction with the Green-Kubo method and the Evans-Gillan[9,10] NEMD method are discussed. The results are given in Sec. V and the conclusions of this study are given in Sec. VI.

II. MODEL AND SIMULATION PARAMETERS

The BMHTF rigid ion interionic potential has the following form:

$$u_{ij}(r) = \frac{Z_i Z_j e^2}{r} + A_{ij}\exp[B(\sigma_i+\sigma_j-r)] - \frac{C_{ij}}{r^6} - \frac{D_{ij}}{r^8}, \quad (1)$$

where the first term is the Coulombic interaction, the second the Born-Huggins exponential repulsion with parameters obtained by Tosi and Fumi,[7,8] and the third and fourth terms are, respectively, the dipole-dipole and dipole-quadrupole dispersion energies with parameters obtained by Mayer.[6]

The Ewald sum method was used to calculate the Coulombic potential energy and forces.[11] For the simulations reported here the value of the convergence parameter η in the Ewald sum was set equal to $5.6/L$ with a truncation of the real part of the Ewald-Coulomb potential at $r_c=L/2$ and the reciprocal space part of the force and potential energy was summed up to the vector $|\mathbf{h}|^2_{\max}=27$, with the k-space vector given by $\mathbf{k}=2\pi\mathbf{h}/L$. The simulations were performed in the canonical ensemble with a Gaussian thermostat, for a cubic sample composed of $N=216$ ions (108 cations and 108 anions) using periodic boundary conditions and the minimum image convention. The positions at time zero were defined as those corresponding to the face-centred cubic lattice of solid NaCl and the zero time velocities were defined randomly and scaled to ensure a zero total linear momentum. A Gear fifth-order algorithm for first-order differential equations was used to solve the equations of motion[12] with a time step of 1.0 fs. The NEMD thermal conductivity, λ, was calculated from simple block averages of 10 000 time steps each from 1.5×10^6 time-step (1.5 ns) production runs after 1.5×10^5 (0.15 ns) time-step equilibration runs. The energy and charge autocorrelation functions and the energy-charge cross-correlation function used to obtain the Green-Kubo EMD thermal conductivity were calculated from at least 3.5×10^6 time-step (3.5 ns) production runs after 1.5×10^5 time-step (0.15 ns) equilibration runs. The thermal conductivity was calculated at five different temperatures; the volume at each temperature was calculated from experimental liquid density data correlations.[13]

III. PHENOMENOLOGICAL RELATIONS

In this section we derive relations for the thermal conductivity and the Seebeck coefficient for a binary ionic mixture from irreversible thermodynamics. The relations discussed here are given for a binary system for which no viscous forces, external magnetic fields, or electronic currents occur and no chemical reactions take place between its components.

A. Thermal conductivity

The entropy production, σ, for a binary ionic mixture is given by the sum of three terms each being the product of a nonconvective flux and the corresponding thermodynamic force.[2,14] These are, respectively, the fluxes of heat, $\mathbf{J}_Q$, mass (of a given component 1), $\mathbf{J}_1$, and charge, $\mathbf{J}_Z$, and the gradients of temperature, chemical potential, and electrostatic potential, i.e.,

$$\sigma = -\frac{1}{T^2}\mathbf{J}_Q\cdot\nabla T - \frac{1}{T}\mathbf{J}_1\cdot\nabla_T(\mu_1-\mu_2) + \frac{1}{T}\mathbf{J}_Z\cdot\mathbf{E}, \quad (2)$$

where $\mathbf{J}_1=-\mathbf{J}_2$ and $\mathbf{J}_Z=\mathbf{J}_1(z_1-z_2)$; $z_\alpha=Z_\alpha/m_\alpha$ is the charge per unit of mass of component α. In Eq. (2) ∇T is the temperature gradient, $\nabla_T\mu_{\alpha=1,2}$ is the chemical potential gradient (to be taken at constant T) of component α, and $\mathbf{E}=-\nabla\phi$ is the external electric field. In order to calculate the thermal conductivity of a binary ionic mixture from the appropriate phenomenological laws, we first redefine the entropy production of Eq. (2) in a more convenient form. This can be done, by introducing the electrochemical potential of component α, μ^Z_α, given by,

$$\mu^Z_\alpha = \mu_\alpha + z_\alpha\phi. \quad (3)$$

The entropy given in Eq. (2) can be transformed through substitution for μ_α from Eq. (3) to give

$$\sigma = -\frac{1}{T^2}\mathbf{J}_Q\cdot\nabla T - \frac{1}{T}\mathbf{J}_Z\cdot\nabla_T\mu_Z, \quad (4)$$

where $\mu_Z=(\mu^Z_1-\mu^Z_2)/(z_1-z_2)$. The phenomenological laws that express the two fluxes of Eq. (4) are[2]

$$\mathbf{J}_Q = -\frac{L^1_{QQ}}{T^2}\nabla T - \frac{L^1_{QZ}}{T}\nabla_T\mu_Z,$$
$$\mathbf{J}_Z = -\frac{L^1_{ZQ}}{T^2}\nabla T - \frac{L^1_{ZZ}}{T}\nabla_T\mu_Z, \quad (5)$$

where $L^1_{\alpha\beta}$ $(\alpha,\beta=Z,Q)$ are the phenomenological coefficients. From Onsager's reciprocal relations[15] for the cross coefficients, $L^1_{ZQ}=L^1_{QZ}$, and thus only three independent coefficients are involved in Eq. (5). The elimination of $\nabla_T\mu_Z$, through $\mathbf{J}_Z$, in the equation for $\mathbf{J}_Q$ allows one to rewrite the heat flux in the following form:[16]

$$\mathbf{J}_Q = \frac{L^1_{QZ}}{L^1_{ZZ}}\mathbf{J}_Z - \lambda^1 \nabla T, \tag{6}$$

where λ^1 is the thermal conductivity corresponding to a situation of zero electric current, $\mathbf{J}_Z=0$, given by

$$\lambda^1 = \frac{1}{T^2}\left(L^1_{QQ} - \frac{L^{1\,2}_{QZ}}{L^1_{ZZ}}\right). \tag{7}$$

The reciprocal relation $L^1_{ZQ}=L^1_{QZ}$ was used to derive this equation. Notice that for $\mathbf{J}_Z=0$, Eq. (6) becomes the Fourier law of heat conduction, $\mathbf{J}_Q=-\lambda^1\nabla T$. Moreover, L^1_{ZZ}/T can be identified as the electrical conductivity, κ, defined as the ratio between the electric current density, $\mathbf{J}_Z$, and the negative gradient of μ_Z under isothermal conditions, $\nabla T=0$.[17] For constant chemical potential, Ohm's law, $\mathbf{J}_Z=\kappa\mathbf{E}$, is obtained by separating the electrochemical potential into its chemical and electrical parts.

The thermal conductivity of a molten alkali halide treated as a binary ionic mixture can in principle be calculated from Eq. (7). However, for reasons discussed below it is preferred for simulation purposes to define the thermal conductivity in terms of the energy flux, $\mathbf{J}_E=\mathbf{J}^0_Q$, rather than the heat flux. Introducing the quantity $h^Z_\alpha=h_\alpha+z_\alpha\phi$ where h_α is the partial specific enthalpy of component α, and using the following relation between the two fluxes:

$$\mathbf{J}^0_Q = \mathbf{J}_Q + \sum_{\alpha=1}^{2} h^Z_\alpha \mathbf{J}_\alpha = \mathbf{J}_Q + h_Z\mathbf{J}_Z, \tag{8}$$

we find the following modified relation for the entropy production:

$$\sigma = -\frac{1}{T^2}\mathbf{J}^0_Q \cdot \nabla T - \mathbf{J}_Z \cdot \nabla\left(\frac{\mu_Z}{T}\right), \tag{9}$$

where the thermodynamic relation

$$T\nabla\left(\frac{\mu_Z}{T}\right) = \nabla_T\mu_Z - \frac{h_Z}{T}\nabla T \tag{10}$$

was used with $h_Z=(h^Z_1-h^Z_2)/(z_1-z_2)$ and we have used the fact that for a binary mixture $\mathbf{J}_1=-\mathbf{J}_2$ and $\mathbf{J}_Z=\mathbf{J}_1(z_1-z_2)$. This transformation of the entropy production is possible due to the fact that there is no unique way of splitting the heat transported by pure heat conduction and the heat transported as a result of the diffusion of the particles of the system.[14]

The phenomenological equations corresponding to Eq. (9) are

$$\begin{aligned}\mathbf{J}^0_Q &= -\frac{L^0_{QQ}}{T^2}\nabla T - L^0_{QZ}\nabla\left(\frac{\mu_Z}{T}\right),\\ \mathbf{J}_Z &= -\frac{L^0_{ZQ}}{T^2}\nabla T - L^0_{ZZ}\nabla\left(\frac{\mu_Z}{T}\right).\end{aligned} \tag{11}$$

We are interested in expressing the thermal conductivity given by Eq. (6) in terms of the phenomenological coefficients, $L^0_{\alpha\beta}$, that appear in Eqs. (11). Applying the transformation given by Eqs. (8) and (10) to the phenomenological equations, Eq. (5), one finds the following relations between the two sets of phenomenological coefficients, $L^1_{\alpha\beta}$ and $L^0_{\alpha\beta}$:

$$\begin{aligned}L^1_{ZZ} &= L^0_{ZZ},\\ L^1_{ZQ} &= L^1_{QZ} = L^0_{ZQ} - h_Z L^0_{ZZ},\\ L^1_{QQ} &= L^0_{QQ} - 2L^0_{QZ}h_Z + L^0_{ZZ}h^2_Z,\end{aligned} \tag{12}$$

and upon substitution in Eq. (7) for the thermal conductivity, λ^1,

$$\lambda^1 = \frac{1}{T^2}\left(L^0_{QQ} - \frac{L^{0\,2}_{QZ}}{L^0_{ZZ}}\right). \tag{13}$$

Thus, the thermal conductivity can be calculated from the coefficients, $L^0_{\alpha\beta}$, which in turn can be obtained through MD simulations. Moreover it can be seen that the electrical conductivity is now given by L^0_{ZZ}/T. Notice that Eq. (13) corresponds to a situation of zero electric current, $\mathbf{J}_Z$, and therefore from Eq. (8), $\mathbf{J}^0_Q=\mathbf{J}_Q$.

B. Seebeck coefficient

As mentioned in the Introduction, the experimental study of the so-called thermal diffusion potentials (the potential difference which arises as a consequence of a temperature and concentration gradient) of electrolytes can be performed through the measurement of the thermoelectric power of a thermocell.[2] In the thermocell, the application of a temperature gradient to a solid or molten salt, or any electrolyte solution in general, causes a redistribution of the particles of the system (due to the different mobility of the ions) resulting in an electrical potential gradient. That potential, together with other potential differences, can be measured across the condensor plates of the cell in the stationary state of vanishing electric current. According to Eq. (5), the steady state of zero electric current for a binary ionic mixture is related to the balance $(L^1_{ZQ}/T^2)\nabla T=(L^1_{ZZ}/T)\nabla_T\mu_Z$.

If the electrolyte in the thermocell is a solution (e.g., aqueous NaCl solution), then the temperature difference gives rise to thermal diffusion and ultimately to some degree of separation of the solute and solvent (and associated potential gradient). As this separation proceeds, the gradient of electrical potential changes towards an equilibrium value characteristic of the final steady state. In this case the thermoelectric power can be measured either under conditions in which no separation of the solute and solvent can occur in the course of the experiment, thus giving the initial thermoelectric power, or during the establishment of the Soret equilibrium.[18]

The potential difference measured for a specific thermocell is the sum of three terms: (i) the homogeneous potential difference, ΔV_{hom}, due to the temperature gradient applied to the electrolyte, (ii) the sum of the contact potential differences at the electrode-electrolyte interfaces, ΔV_{hel}, and (iii) the sum of the homogeneous potential differences within the metal wires. The magnitude of this third term is normally small compared with the first two and it is neglected. Hence the thermoelectric power of the thermoelectric cell is given by

$$\theta = \frac{\Delta V_{\text{hom}}}{\Delta T} + \frac{\Delta V_{\text{het}}}{\Delta T} = \alpha + \frac{\Delta V_{\text{het}}}{\Delta T}. \tag{14}$$

From the previous discussion one can define the homogeneous Seebeck coefficient or thermoelectric power, α, of a binary ionic mixture as the electric field induced by a temperature gradient, at zero electric current. Hence, from Eq. (5) for $\mathbf{J}_Z$ we have

$$\nabla_T \mu_Z = -\alpha \nabla T, \tag{15}$$

where

$$\alpha = \frac{L^1_{ZQ}}{L^1_{ZZ} T}. \tag{16}$$

For constant chemical potential, separating the electrochemical potential into its chemical and electrical parts, Eq. (15) becomes, $\mathbf{E} = \alpha \nabla T$. As for the case of the thermal conductivity coefficient, we are interested in expressing the homogeneous Seebeck coefficient in terms of the coefficients, $L^0_{\alpha\beta}$. Through the relations given above between the two sets of coefficients given in Eq. (12), we find

$$\alpha = \frac{L^0_{ZQ} - h_Z L^0_{ZZ}}{L^0_{ZZ} T}. \tag{17}$$

Hence, unlike thermal conductivity, the Seebeck coefficient involves h_Z, which is very difficult to obtain through MD simulations. In this work we could not calculate this term and we limit the discussion to the term $\alpha^h = \alpha + h_Z/T = L^0_{ZQ}/(L^0_{ZZ}T)$ obtained for molten NaCl and KCl.

IV. SIMULATION METHODS

A. EMD Green-Kubo method

The three phenomenological coefficients involved in Eqs. (13) and (17) can be obtained through equilibrium molecular dynamics (EMD) simulations in conjunction with the Green-Kubo method. The phenomenological coefficients are given by the following Green-Kubo integral:

$$L_{\alpha\beta} = \frac{1}{3k_B V} \int_0^\infty \langle \mathbf{j}_\alpha(t) \cdot \mathbf{j}_\beta(0) dt \rangle. \tag{18}$$

For convenience we redefine the phenomenological coefficients in the following way:

$$L^0_{ZZ} = L_{ZZ} T,$$

$$L^0_{QZ} = L_{EZ} T^2, \tag{19}$$

$$L^0_{QQ} = L_{EE} T^2,$$

thereby giving the following equations for the three phenomenological coefficients:

$$L_{ZZ} = \frac{1}{3Vk_B T} \int_0^\infty \langle \mathbf{j}_Z(t) \cdot \mathbf{j}_Z(0) \rangle dt,$$

$$L_{EZ} = \frac{1}{3Vk_B T^2} \int_0^\infty \langle \mathbf{j}_E(t) \cdot \mathbf{j}_Z(0) \rangle dt, \tag{20}$$

$$L_{EE} = \frac{1}{3Vk_B T^2} \int_0^\infty \langle \mathbf{j}_E(t) \cdot \mathbf{j}_E(0) \rangle dt,$$

where $L_{ZZ} = \kappa$ is the electrical conductivity, L_{EZ} is a cross thermoelectric coefficient, and L_{EE} would correspond to the thermal conductivity of a neutral one-component fluid. With these definitions Eqs. (13) and (17) become

$$\lambda = L_{EE} - \frac{L^2_{EZ} T}{L_{ZZ}},$$

$$\alpha^h = \frac{L_{EZ}}{L_{ZZ}}. \tag{21}$$

In Eq. (20) $\mathbf{j}_Z$ and $\mathbf{j}_E$ are, respectively, the microscopic fluxes of charge and energy given by (for zero barycentric velocity, $\mathbf{u}$)

$$\mathbf{j}_Z = \sum_{i=1}^N Z_i e \mathbf{v}_i(t),$$

$$\mathbf{j}_E = \mathbf{j}_Q + \sum_i^N \nu_i h_i = \frac{1}{2} \sum_{i=1}^N \left[m_i \nu_i^2 + \sum_{j \neq i}^N u(r_{ij}) \right] \mathbf{v}_i + \frac{1}{2} \sum_{i=1}^N \sum_{j \neq i}^N (\mathbf{r}_{ij} \mathbf{F}_{ij}) \cdot \mathbf{v}_i, \tag{22}$$

where $\mathbf{v}_i$ is the velocity of particle i, $u(r_{ij})$ the pair potential between particles i and j, $\mathbf{r}_i$ the position vector of particle i, and h_i is the partial enthalpy per particle.[19,20] For simplicity the microscopic fluxes were written for a pure fluid, with the understanding that the sums are to be performed over two different species ($N = 2N_+ = 2N_-$). The reason for applying the transformation of Eq. (8) to the macroscopic heat flux (also valid for the microscopic currents) is to avoid the calculation of the partial enthalpy per particle of the two ionic species, h_i, which appears in the definition of the microscopic flux of heat, $\mathbf{j}_Q$. For zero total linear momentum (but only for a one-component system) this term is zero due to conservation of linear momentum and $\mathbf{j}_E = \mathbf{j}_Q$. For mixtures this enthalpy term is different from zero and except for the case of ideal mixtures it cannot be neglected. This is also the reason why the calculation of the thermal conductivity of mixtures through the Evans-Gillan algorithm is very difficult. The problem lies in the lack of a microscopic expression for the partial enthalpy h_α that appears in Eq. (8). For the case of a real binary mixture the partial enthalpy can be obtained in an approximate form from the difference between the enthalpy calculated through two isobaric, isothermal simulations in which the composition of the system is changed by addition or removal of a single particle. For the special case of a binary ionic mixture, the partial enthalpy cannot be calcu-

lated by strict application of this thermodynamic definition,

$$h_\alpha = \left(\frac{\partial H}{\partial N_\alpha}\right)_{T,P,N_\beta} \tag{23}$$

without violation of the electroneutrality condition. We note, however, that Debenedetti[21] has proposed a fluctuation-based method to obtain partial molar volumes, energies, and enthalpies in the microcanonical ensemble from a single simulation. Through this method it is possible to calculate the property not as a difference but via a computer simulation of the appropriate fluctuations. Although this method has not been extended to the (N,P,T) ensemble it is of special interest for the case of molten salts since the method only involves the possible loss of local electroneutrality. We have not, however, in this study, investigated this approach and we simply neglect the enthalpic term both for the calculation of the thermal conductivity through NEMD simulations and on the calculation of the homogeneous Seebeck coefficient.

Finally and following the discussion of Galamba *et al.*[3] we note that the potential part of Eq. (22) for the microscopic flux of energy of Ewald-Coulomb systems is not valid for the calculation of the reciprocal space part of this term. The reason is that the reciprocal space part of the Ewald-Coulomb forces is not pairwise additive and therefore the whole term must be calculated in the reciprocal space. Hence, the microscopic flux of energy for Ewald-Coulomb systems is given by

$$\mathbf{j}_E = \frac{1}{2}\sum_{i=1}^{N}\left[m_i v_i^2 + \sum_{j\neq i}^{N} u(r_{ij})\right]\mathbf{v}_i + \frac{1}{2}\sum_{i=1}^{N}\sum_{j\neq i}^{N}(\mathbf{r}_{ij}\mathbf{F}_{ij}^R)\cdot\mathbf{v}_i + \frac{1}{2}\sum_{i=1}^{N}\sum_{j=1}^{N}\mathbf{v}_i\cdot\mathbf{S}_{ij}, \tag{24}$$

with

$$\mathbf{S}_{ij}^{\alpha\beta} = \frac{4\pi}{L^3}\sum_{\mathbf{k}\neq 0}^{\infty} B_{\alpha\beta}\frac{1}{k^2}e^{-k^2/4\eta^2}Z_iZ_j\cos(\mathbf{k}\cdot\mathbf{r}_{ij}) \tag{25}$$

and for the $\alpha\beta$ component of the tensor $\mathbf{B}(\mathbf{k})$,

$$B_{\alpha\beta} = \delta_{\alpha\beta} - \frac{2|\mathbf{k}_\alpha||\mathbf{k}_\beta|}{|\mathbf{k}|^2} - \frac{|\mathbf{k}_\alpha||\mathbf{k}_\beta|}{2\eta^2}, \tag{26}$$

where η is the convergence parameter of the Ewald sum, and $\delta_{\alpha\beta}$ is the Kronecker delta. In Eq. (24) $\mathbf{F}_{ij}^R$ represents the short-range forces and the real part of the Ewald-Coulomb forces, both computed in the real space.

B. NEMD method

The NEMD method used in this work was that of Evans and Gillan.[9,10] The driving force in this algorithm is a fictitious heat field vector $\mathbf{F}_Q$, which generates a heat flux $\mathbf{J}_Q$. The equations of motion are of the following form:[22]

$$\dot{\mathbf{r}}_i = \frac{\mathbf{p}_i}{m},$$

$$\dot{\mathbf{p}}_i = \mathbf{F}_i + (E_i - E)\mathbf{F}_Q(t) + \frac{1}{2}\sum_{j=1}^{N}\mathbf{F}_{ij}(\mathbf{r}_{ij}\cdot\mathbf{F}_Q(t)) - \frac{1}{2N}\sum_{j,k}^{N}\mathbf{F}_{jk}(\mathbf{r}_{jk}\cdot\mathbf{F}_Q(t)) - \xi\mathbf{p}_i, \tag{27}$$

where ξ is the Gaussian thermostat multiplier given by

$$\xi = \frac{\sum_{i=1}^{N}\left[\mathbf{p}_i/m_i\cdot\left(\mathbf{F}_i + (E_i - E)\mathbf{F}_Q(t) + \frac{1}{2}\sum_{j=1}^{N}\mathbf{F}_{ij}(\mathbf{r}_{ij}\cdot\mathbf{F}_Q(t)) - \frac{1}{2N}\sum_{j,k}^{N}\mathbf{F}_{jk}(\mathbf{r}_{jk}\cdot\mathbf{F}_Q(t))\right)\right]}{\sum_{i=1}^{N}p_i^2/m_i}. \tag{28}$$

Following common practice[22] $\mathbf{F}_Q$ was chosen to act in the z direction. The equations of motion, Eq. (27), drive a heat current in the direction of the external field and the thermal conductivity is calculated from

$$\lambda = \frac{\langle j_Q^z\rangle}{TVF_Q}, \tag{29}$$

where j_Q^z is the z component of the heat flux vector. Following Evans and Morriss' discussion,[22] even though we use λ in Eq. (29) and refer to it hereinafter as the thermal conductivity, we stress that there is no reason to identify λ (F_Q) with the nonlinear thermal conductivity λ (∇T). Hence, only in the limit $F_Q \to 0$ can λ be identified with the thermal conductivity.

The algorithm given above is only valid for the case of one-component systems in the sense that it does not allow one to obtain all three independent phenomenological coefficients associated with the coupled fluxes of heat and mass that take place in neutral binary mixtures. Hence, this algorithm must be generalized to the case of binary mixtures even if we are only interested in the calculation of the thermal conductivity. Such generalization has been proposed by

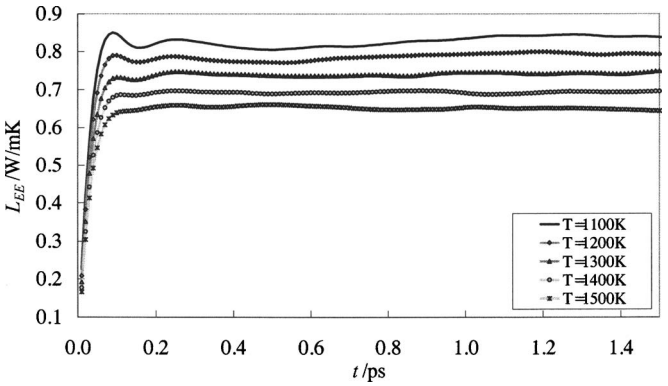

FIG. 1. L_{EE} coefficient obtained from Green-Kubo EMD (N,V,T) simulations of the BMHTF interionic potential for NaCl at five different state points.

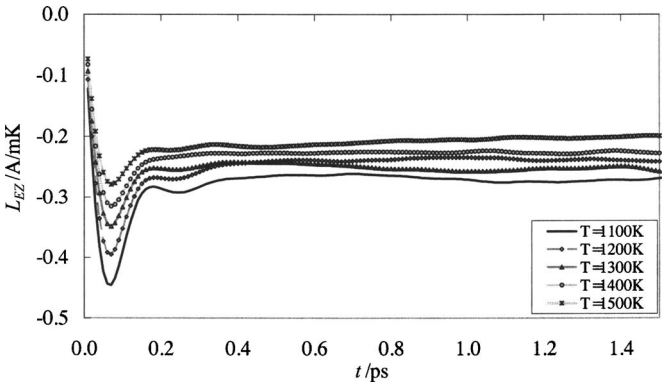

FIG. 3. L_{EZ} coefficient obtained from Green-Kubo EMD (N,V,T) simulations of the BMHTF interionic potential for NaCl at five different state points.

MacGowan and Evans[23] for the case of binary mixtures. That approach can be extended to the case of binary ionic mixtures, but the problem of obtaining the partial enthalpy for the mixture's components from the same set of simulations is unresolved.[24] Thus, in this work the algorithm for a one-component fluid was used. The two approximations involved in this approach are

$$\lambda^1 = \frac{1}{T^2}\left(L_{QQ}^1 - \frac{L_{QZ}^{1\,2}}{L_{ZZ}^1}\right) \approx \frac{1}{T^2}L_{QQ}^1 = L_{QQ},$$

$$L_{QQ} = \frac{\langle j_Q^z \rangle}{TVF_Q} \approx \frac{\langle j_E^z \rangle}{TVF_Q}. \tag{30}$$

The results obtained through NEMD simulations must therefore be interpreted in the light of these approximations.

V. RESULTS

Figures 1–3 display the coefficients L_{EE}, L_{ZZ}, and L_{EZ} for the BMHTF model of NaCl at five different temperatures obtained from Green-Kubo EMD simulations. For KCl, similar plots (not displayed here) were obtained for L_{EE} and L_{ZZ}. Figure 4 shows the cross thermoelectric coefficient, L_{EZ}, for KCl. Analysis of the EMD results allow one to establish the following relations for the three phenomenological coefficients: (i) L_{EE} decreases with increasing temperature and $L_{EE,\mathrm{NaCl}} > L_{EE,\mathrm{KCl}}$, (ii) L_{ZZ} increases with the increasing temperature and $L_{ZZ,\mathrm{NaCl}} > L_{ZZ,\mathrm{KCl}}$, and (iii) L_{EZ} is negative for NaCl and positive for KCl; $|L_{EZ}|$ decreases with the increase of temperature and $|L_{EZ,\mathrm{NaCl}}| \gg |L_{EZ,\mathrm{KCl}}|$.

The cross thermoelectric coefficient, L_{EZ}, is the most difficult to obtain with high statistical precision and deviations can be observed from the general temperature dependence (see Figs. 3 and 4). We believe that these deviations result from the low signal-to-noise ratios involved in the Green-Kubo method in addition to the weak temperature dependence of this coefficient. A particularly interesting result obtained in this study concerns the opposite sign of L_{EZ} for molten NaCl and KCl. From a molecular point of view, differences between NaCl and KCl result from the different forces experienced by the ions and the different sizes and masses of the cations. These microscopic differences allow one to explain certain differences in the macroscopic property behavior of the two molten salts. For the specific case of the inversion of sign of L_{EZ}, we can show that this behavior is closely related to the relation between the masses of the positive and negative ions, i.e., for NaCl $m_+ > m_-$ and for KCl $m_+ < m_-$.

To allow a full understanding of this effect we have interchanged the mass of Na^+ and Cl^- and calculated the cross thermoelectric coefficient for this model system referred to herein as ClNa. The cross coefficient of NaCl is compared to

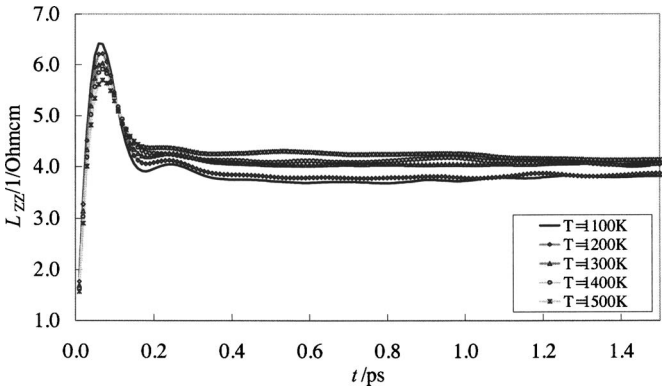

FIG. 2. L_{ZZ} coefficient obtained from Green-Kubo EMD (N,V,T) simulations of the BMHTF interionic potential for NaCl at five different state points.

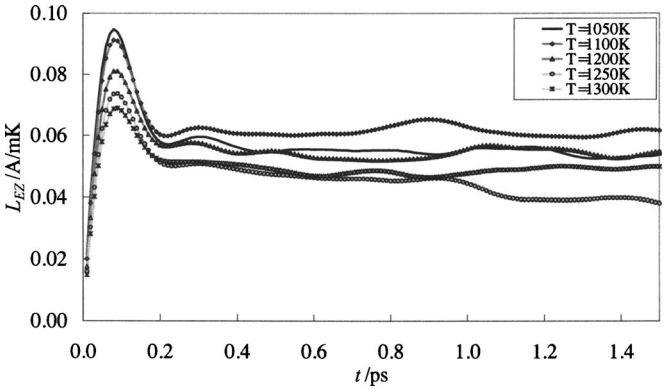

FIG. 4. L_{EZ} coefficient obtained from Green-Kubo EMD (N,V,T) simulations of the BMHTF interionic potential for KCl at five different state points.

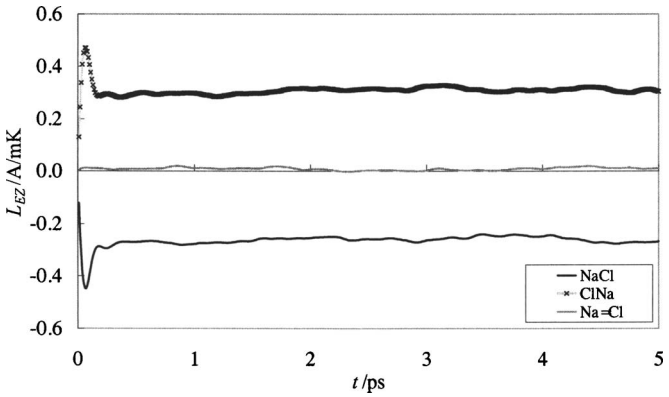

FIG. 5. Thermoelectric cross coefficient L_{EZ} for NaCl, ClNa, and Na=Cl according to the definitions given in the text.

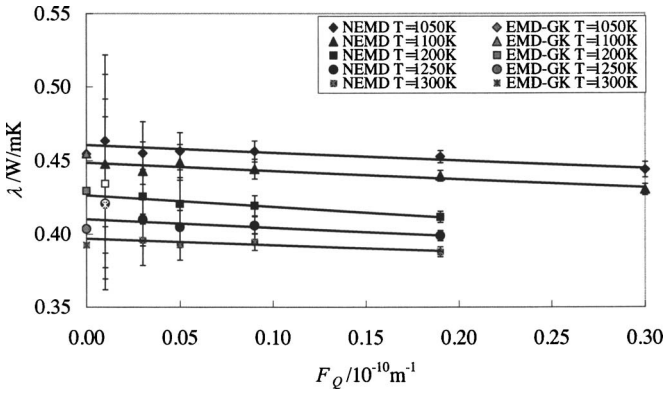

FIG. 7. Thermal conductivity for the BMHTF model of KCl obtained from NEMD and Green-Kubo (GK) EMD simulations. The points with white background were neglected in the least squares fits.

that of ClNa in Fig. 5. Further we have calculated the cross thermoelectric coefficient for the case where the mass of the Na^+ is equal to the mass of a Cl^- ion. This system is denoted by Na=Cl in Fig. 5. From Fig. 5 the effect of the mass on the cross thermoelectric coefficient L_{EZ} is clear. For the special case of Na=Cl the coefficient is zero and thus it does not contribute to the thermal conductivity of the "model fluid" in analogy with the case of a pure fluid. Notice that in spite of the fact that the masses of the two ionic species are the same, three different interactions still take place. On the other hand the fact that the cross thermoelectric coefficient is about five times higher for NaCl than for KCl can also be attributed almost exclusively to the cationic mass differences. Also note that L_{EZ} for ClNa is not exactly symmetric to the same coefficient for the NaCl case. The reason is that even though the masses were interchanged, the interactions between the ions are exactly the same as those of NaCl.

Based on these results one can obtain some insight into the structural response of a molten alkali halide to a temperature gradient. Repositioning of the positive and negative species relative to the "hot" and "cold" parts of the system seems to depend almost exclusively on their masses. Due to the difficulties referred to above concerning the calculation of the homogeneous Seebeck coefficient, one cannot, however, make any conclusions concerning the sign of this coefficient. The experimental values of θ reported by Detig and Archer[25] for pure molten NaCl and KCl at 860 °C (1133 K) and 830 °C (1103 K), respectively, are $\theta_{NaCl}=-0.45$ mV/°C and $\theta_{KCl}=-0.40$ mV/°C. The contribution from the homogeneous thermoelectric potential characteristic of the molten salts is not known.

We now turn attention to the results obtained through NEMD simulations. Figures 6 and 7 compare the "thermal conductivity" obtained from NEMD simulations with the equilibrium thermal conductivity obtained through Green-Kubo EMD simulations. Given the two approximations defined in Eq. (30), the agreement observed between the NEMD and the EMD simulated thermal conductivities is somewhat unexpected, especially for the case of molten NaCl. We advance two possible reasons that may explain this result: (i) cancellation effects between the omitted enthalpy contribution to the microscopic heat flux and the subtracted term, TL_{QZ}^2/L_{ZZ}, in the definition of λ for a binary ionic mixture, or (ii) NEMD is significantly less system size dependent and more precise than the Green-Kubo method.

The first implies that the enthalpy term in the heat flux vector causes a contribution to the thermal conductivity comparable to TL_{QZ}^2/L_{ZZ} but of opposite sign. The later assumes that the Green-Kubo EMD thermal conductivity is overpredicted due to system size dependence of the method. Furthermore, because of the low statistical precision of the Green-Kubo method, it is very difficult to estimate the accuracy of the results for a specific number of particles. The NEMD

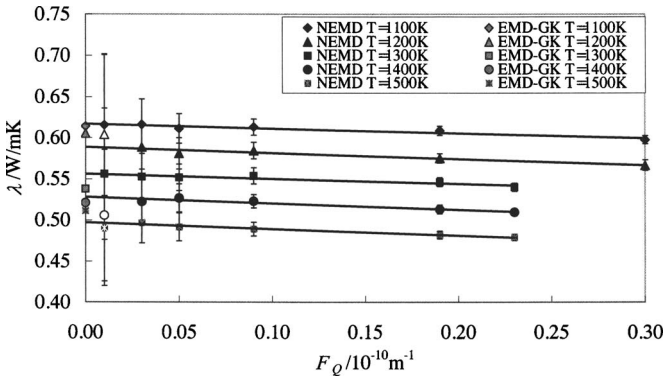

FIG. 6. Thermal conductivity for the BMHTF model of NaCl obtained from NEMD and Green-Kubo (GK) EMD simulations. The points with white background were neglected in the least squares fits.

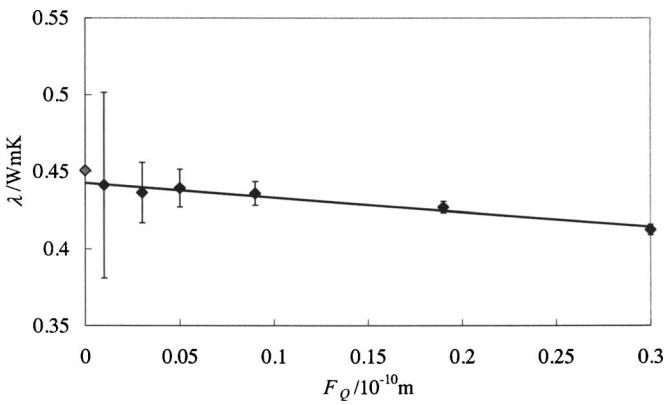

FIG. 8. Thermal conductivity for Na=Cl obtained from NEMD and Green-Kubo (GK) EMD simulations at $T=1100$ K.

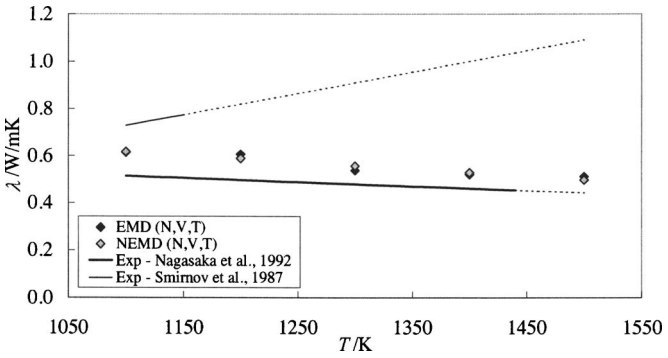

FIG. 9. Comparison between the Green-Kubo EMD and NEMD thermal conductivity for NaCl obtained in this work with experimental data. The dashed lines were obtained through extrapolation of the corresponding experimental correlation equations, up to the highest simulation temperature investigated in this study.

simulations in turn are more precise (for large values of the fictitious heat field, F_Q), but involve an extrapolation to $F_Q=0$ to obtain the thermal conductivity.

To explore these two possibilities we have calculated the thermal conductivity of Na=Cl using NEMD for which the approximations given in Eq. (30) disappear and then compare the results to $\lambda=L_{EE}$ obtained through Green-Kubo EMD for this system. If hypothesis (i) is correct and (ii) is incorrect, we expect that the agreement between the two methods will be good for this system, since in this case there are no approximations involved. If on the other hand the hypothesis (ii) is correct we expect that the thermal conductivity obtained through Green-Kubo EMD will be significantly higher than that computed through the one-component NEMD algorithm. Figure 8 shows the results of these simulations for Na=Cl at a single state point, $T=1100$ K and $\rho=1.5420$ g cm^{-3}. Although the value of λ obtained through Green-Kubo EMD is larger than that obtained from NEMD the difference between the two values is small. Hence, in our opinion, Fig. 8 supports the first hypothesis enunciated above and points to a cancellation between the two approximations expressed by Eq. (30).

Finally we compare our simulation results with available experimental data. Early measurements of the thermal conductivity of molten alkali halides predicted an increase of the thermal conductivity with temperature. Furthermore, differences between different sets of experimental data were often far beyond their claimed accuracy. Nagasaka *et al.*[26] and Nakazawa *et al.*[27,28] measured the thermal diffusivity for 13 molten salts (including NaCl and KCl) from which they calculated the thermal conductivity. The temperature range of these measurements is relatively large and they found considerably lower values for the thermal conductivity than some of the data reported by other authors. In addition, a weak negative temperature dependence was found for the thermal conductivity of every molten salt. Other sets of experimental data have been reported for the thermal conductivity of molten alkali halides, which also show a weak negative temperature dependence. For example, Golyshev *et al.* (1983) reported two data points for the thermal conductivity of NaCl and LiF. Their data predict a negative, close to zero, temperature dependence for the thermal conductivity of these two salts. Harada (personal communication referenced by Nagasaka *et al.*[26]) reported thermal conductivity data for some molten alkali halides that also predicts a weak decrease of the thermal conductivity with temperature. Nagasaka *et al.*[26] and Nakazawa *et al.*[27,28] have compared their experimental data with those studies and good agreement was found.

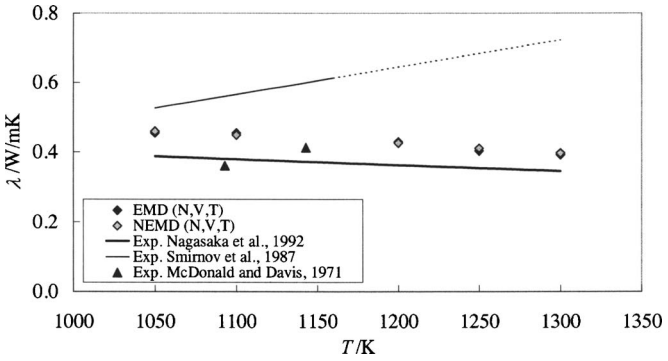

FIG. 10. Comparison between the EMD and NEMD thermal conductivity for KCl obtained in this work with experimental data. The dashed line was obtained through extrapolation of the corresponding experimental correlation equation, up to the highest simulation temperature investigated in this study.

TABLE I. Thermal conductivity of NaCl calculated from Green-Kubo (GK) EMD and NEMD simulations. The experimental results are from Nagasaka *et al.* (Ref. 26).

T (K)	ρ (g cm^{-3})	λ^{NEMD} (W/mK)	λ^{GK} (W/mK)	$\lambda^{Expt.}$ (W/mK)
1100	1.5420	0.617	0.614	0.514
1200	1.4878	0.589	0.605	0.496
1300	1.4335	0.556	0.538	0.478
1400	1.3793	0.528	0.521	0.460
1500	1.3250	0.497	0.511	0.442

Figures 9 and 10 compare the simulation results for the thermal conductivity with different sets of experimental data. The data points of McDonald and Davis[29] for molten KCl are the experimental values reported by the authors. Those of Smirnov *et al.*[30] and Nagasaka *et al.*[26] were calculated from the correlations given by the authors and were extrapolated to allow a comparison with the simulation data for the complete temperature range. The experimental thermal conductivity data of Nagasaka *et al.*[26] have an estimated uncertainty of 8% for both NaCl and KCl. It can be seen that the discrepancies between the experimental data of different authors are large and an opposite temperature dependence is

TABLE II. Thermal conductivity of KCl calculated from Green-Kubo (GK) EMD and NEMD simulations. The experimental results are from Nagasaka *et al.* (Ref. 26).

T (K)	ρ (g cm^{-3})	λ^{NEMD} (W/mK)	λ^{GK} (W/mK)	$\lambda^{Expt.}$ (W/mK)
1050	1.5236	0.460	0.455	0.388
1100	1.4945	0.449	0.455	0.379
1200	1.4362	0.426	0.429	0.362
1250	1.4070	0.410	0.404	0.354
1300	1.3779	0.397	0.393	0.345

TABLE III. Values of the coefficients L_{EZ}, $\kappa=L_{ZZ}$, and α^h obtained from Green-Kubo EMD simulations for NaCl.

T (K)	ρ (g cm^{-3})	L_{EZ} (A/mK)	κ (Ω^{-1} cm^{-1})	α^h (mV/K)
1100	1.5420	−0.268	3.80	−0.704
1200	1.4878	−0.240	3.85	−0.623
1300	1.4335	−0.254	4.11	−0.618
1400	1.3793	−0.226	4.10	−0.555
1500	1.3250	−0.202	4.12	−0.490

predicted. The simulation thermal conductivity is generally overpredicted to within 10%–20% relative to the data of Nagasaka *et al.*[26] and the predicted temperature dependence is weakly negative in agreement with the results from the same authors.

Tables I and II summarize the data for the thermal conductivity of molten NaCl and KCl, respectively obtained through Green-Kubo EMD and NEMD simulations in this study. Tables III and IV give the coefficients L_{EZ}, $\kappa=L_{ZZ}$, and α^h obtained from Green-Kubo EMD simulations, respectively, for NaCl and KCl. Although no experimental correspondence exists for the coefficient α^h it is interesting to notice that the magnitude of this coefficient is reasonable when compared with the experimental overall Seebeck coefficient, θ.

Finally, in Fig. 11 we compare the electrical conductivity, $L_{ZZ}=\kappa$, obtained in this work with experimental electrical conductivity data. The experimental curves given in Fig. 11 were calculated using the NIST molten salt database[13] and were extrapolated up to the minimum and maximum temperature values simulated for fused NaCl and KCl. From Fig. 11 one can see that the simulation results are satisfactory for the two molten salts. Although this paper is not primarily concerned with the electrical conductivity, since the thermal conductivity of binary ionic mixtures depends on the electrical conductivity, the fact that a reasonable result is found for κ is important in determining sources of error in our calculations.

VI. CONCLUSIONS

Equilibrium and nonequilibrium molecular dynamics simulations were carried in the canonical ensemble for the BMHTF rigid ion interionic potential of NaCl and KCl to study the temperature dependence of the thermal conductivity of these materials. The results reported herein are consistent with those published earlier[3] for the same salts and obtained through Green-Kubo EMD simulations in the microcanonical ensemble, i.e., the BMHTF potential over-

TABLE IV. Values of the coefficients L_{EZ}, $\kappa=L_{ZZ}$, and α^h obtained from Green-Kubo EMD simulations for KCl.

T (K)	ρ (g cm^{-3})	L_{EZ} (A/mK)	κ (Ω^{-1} cm^{-1})	α^h (mV/K)
1050	1.5236	0.0547	2.44	0.224
1100	1.4945	0.0614	2.49	0.246
1200	1.4362	0.0540	2.88	0.187
1250	1.4070	0.0429	2.88	0.149
1300	1.3779	0.0483	2.96	0.163

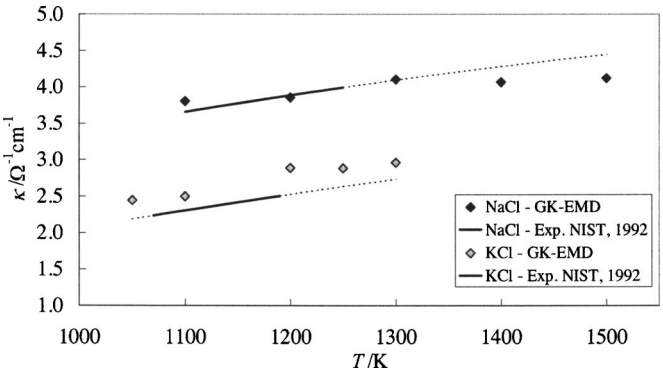

FIG. 11. Comparison between the Green-Kubo EMD electrical conductivity for NaCl and KCl obtained in this work with experimental data. The dashed lines were obtained through extrapolation of the corresponding experimental correlation equations.

predicts the thermal conductivity of both NaCl and KCl compared to that obtained by Nagasaka *et al.*[26] through thermal diffusivity experimental measurements. The results obtained through Green-Kubo EMD for a "binary" ionic mixture and those obtained through homogeneous synthetic NEMD simulations for a one-component fluid were found to be in very good agreement. This result points to a possible cancellation between the enthalpy term omitted in the calculation of the heat flux and the subtracted term in the thermal conductivity definition for a binary ionic mixture related to the coupling between the fluxes of heat and charge.

Further, in this study we have discussed the opposite sign observed for the cross thermoelectric coefficient for molten NaCl and KCl in terms of the masses of the ionic species. Even though it was not possible to calculate the homogeneous Seebeck coefficient through the simulations reported herein this result indicates that the mass of the ionic species plays a fundamental role in the structural response of a binary ionic mixture to a temperature gradient. In future work the thermal conductivity and the homogeneous Seebeck coefficient of these materials will be found through alternative NEMD algorithms that do not require the computation of the microscopic heat flux vector thereby avoiding the difficulties discussed here.

ACKNOWLEDGMENTS

One of the authors (N.G.) would like to acknowledge Ph.D. grant under the program PRAXIS XXI/BD/19792/99, and to Colorado School of Mines, where part of this work was developed, for the opportunity provided as a visiting scholar. Another author (I.F.E.) acknowledges support from the DOE Office of Science, Grant No. DE-FG02-95ER14698.

[1] F. Bresme, B. Hafskjold, and I. Wold, J. Phys. Chem. **100**, 1879 (1996).
[2] S. P. De Groot and P. Mazur, *Non-equilibrium Thermodynamics* (Dover, New York, 1984).
[3] N. Galamba, C. A. N de Castro, and J. F. Ely, J. Chem. Phys. **120**, 8676 (2004).
[4] M. V. Born and I. E. Mayer, Z. Phys. **75**, 1 (1932).
[5] M. L. Huggins and J. E. Mayer, J. Chem. Phys. **1**, 643 (1933).
[6] J. E. Mayer, J. Chem. Phys. **1**, 270 (1933).
[7] M. P. Tosi and F. G. Fumi, J. Phys. Chem. Solids **25**, 45 (1964).
[8] F. G. Fumi and M. P. Tosi, J. Phys. Chem. Solids **25**, 31 (1964).

[9] D. J. Evans, Phys. Lett. **91A**, 457 (1982).
[10] M. J. Gillan and M. Dixon, J. Phys. C **16**, 869 (1983).
[11] M. J. L. Sangster and M. Dixon, Adv. Phys. **25**, 247 (1976).
[12] M. P. Allen and D. J. Tildesley, *Computer Simulations of Liquids* (Clarendon, Oxford, 1997).
[13] G. J. Janz, Database NIST Properties of Molten Salts Database (NIST SRD 27, Boulder, 1992).
[14] H. J. M. Hanley, *Transport Phenomena in Fluids* (Dekker, New York, 1969).
[15] L. Onsager, Phys. Rev. **37**, A405 (1931).
[16] B. Bernu and J. P. Hansen, Phys. Rev. Lett. **48**, 1375 (1982).
[17] P. Sindzingre and M. J. Gillan, J. Phys.: Condens. Matter **2**, 7033 (1990).
[18] H. J. V. Tyrrell, *Diffusion and Heat Flow in Liquids* (Butterworths, London, 1961).
[19] R. Zwanzig, Annu. Rev. Phys. Chem. **16**, 67 (1965).
[20] D. A. McQuarrie, *Statistical Mechanics* (Harper and Row, New York, 1976).
[21] P. G. Debenedetti, J. Chem. Phys. **86**, 7126 (1987).
[22] D. J. Evans and G. P. Morriss, *Statistical Mechanics of Nonequilibrium Liquids* (Academic, London, 1990).
[23] D. MacGowan and D. Evans, Phys. Rev. A **34**, 2133 (1986).
[24] D. Evans and D. MacGowan, Phys. Rev. A **36**, 948 (1987).
[25] R. H. Detig and D. H. Archer, J. Chem. Phys. **38**, 661 (1963).
[26] Y. Nagasaka, N. Nakazawa, and A. Nagashima, Int. J. Thermophys. **13**, 555 (1992).
[27] N. Nakazawa, Y. Nagasaka, and A. Nagashima, Int. J. Thermophys. **13**, 753 (1992).
[28] N. Nakazawa, Y. Nagasaka, and A. Nagashima, Int. J. Thermophys. **13**, 763 (1992).
[29] J. McDonald and H. T. Davis, Phys. Chem. Liq. **2**, 119 (1971).
[30] M. V. Smirnov, V. A. Khokhlov, and E. S. Filatov, Electrochim. Acta **32**, 1019 (1987).